

Blade Property Measurement and Its Assessment on Air/Structural Loads of HART II Rotor¹

Sung N. Jung,* Young H. You, Manoj K. Dhadwal
Dept. of Aerospace Information Engineering
Konkuk University, South Korea

Brandon P. Hagerty
NASA Ames Research Center
Moffett Field, California

Johannes Riemenschneider, Ralf Keimer
German Aerospace Center
38108 Braunschweig, Germany

I. Research Background

An international collaborative research program, HART (Higher-harmonic-control Aeroacoustic Rotor Test) II [1], was conducted in 2001 in the open-jet anechoic test chamber of the German-Dutch wind tunnel (DNW) by a joint research team from the German DLR, the French ONERA, NASA Langley, DNW, and the U.S. Army. A variety of up-to-date test techniques were employed to measure the airloads, vortex trajectories, blade motions, noise levels, and structural moments with and without higher harmonic control (HHC) pitch inputs. After the test, a significant volume of research has been carried out worldwide to validate the test data using various analytical and numerical tools and to gain more physical insights into the blade-vortex interaction behavior of a rotor particularly in a descending flight [2]. It is no doubt that the HART II program results in a remarkable success in the rotorcraft aeromechanics fields and contributes significantly to the advancement of the prediction capability. However, all the previous validation efforts associated with HART II rotor are fundamentally based on the blade section properties obtained by MBB (Messerschmitt-Bölkow-Blohm), manufacturer of the HART II blades, using a two-dimensional finite-element analysis [3]. At the time when the HART II blade property set is released to the public, some additional adjustments of the section property set have been made to better match the test data. Other than this earlier attempt, no other serious action has been taken so far to systematically measure the structural properties of HART II blades and to replace the existing fabricated section properties. A recent study on a blade property measurement [4-5] shows that the use of measured blade properties is viable in the rotorcraft aeromechanics analysis to clear or reduce the uncertainty issues existing in the manufacturing stage of blades as opposed to the initial structural layouts and designs, and is essential to reach realistic correlations against the test data. Taking into account of these aspects, a careful measurement of HART II blade structural properties should be performed to provide the high-precision measured properties as well as to identify the impact of new property set in the aeromechanics analysis of the rotor in comparison with those by the previously-fabricated properties.

¹ Suggested for presentation at the AHS International 70th Annual Forum & Technology Display, Montréal, Québec, Canada, May 20-22, 2014.

The present study focuses to measure the structural properties of HART II blades for the first time since the wind tunnel test of HART II rotor in 2002. The original set of HART II rotor consists of a total of four blades including a pressure sensor-instrumented blade (Figure 1). All the constituent blades are equipped with strain gages to evaluate the structural loads of the rotor. One spare blade is also manufactured for redundancy purpose. Both the instrumented blade and the spare blade are used in the present study for the measurement of structural properties. However, since these blades are intact and clean, and thus no destructive testing is allowed for possible use in the future, an additional blade having equivalent structural properties is introduced for physical cutting (chopping) of blades. In summary, three blades are used for the present measurement activity: instrumented HART II blade (H2A), spare HART II blade (H2S), and HART II-equivalent blade (H2E). Each of the blades is shown in Figure 2. This activity is resulted from an international joint effort through research collaboration between NASA Ames, DLR (German Aerospace Center), and Konkuk University.

II. Objectives

The major goal of the present study is to conduct the measurement of structural properties of HART II blades, to provide a unified version of measured blade property table to the rotorcraft community, and also to replace the existing set of fabricated property table. The measurements include bending and torsion stiffness, geometric offsets, and mass and inertia properties of the blade. Besides the conventional mechanical testing methods, several up-to-date test techniques such as the computer tomography coupled with an image processing and the pattern recognition technique are employed for the study [6]. Given the measured blade property set, a comprehensive dynamics evaluation using CAMRAD II [7] is performed to validate the measured data and to evaluate the sensitivity of blade structural properties on airloads and structural loads of HART II rotor. The quality of blade structural measurements is assessed by correlating the comprehensive dynamics predictions against the wind tunnel test data of HART II rotor. Particularly, a stochastic analysis is carried out to identify the relative contribution of individual blade property components on the aeroelastic behavior of the HART II rotor and to determine which part of the update of structural properties has caused what amount of improvement in the aeromechanics predictions.

III. Blade Property Measurements

The testing techniques and procedures for the measurement of HART II blade properties are described in this section. The instrumented blade (H2A) is used to measure the location of elastic axis, flap bending and torsion stiffness, while the mass and inertia properties are obtained using the spare HART II blade (H2S). To cross validate the structural properties, an equivalent HART II blade (H2E) is also introduced. Specially, this H2E blade is chopped into several pieces to obtain the section mass and inertia properties. It is noted that the airfoil section of HART II blade having a constant chord starts at 22% radial station (0.22R) until the blade tip. For convenience, the inboard of 0.22R is called as the blade root section and the

outboard portion as the blade uniform section.

3.1 Elastic axis

The elastic axis is defined as the chordwise position of the blade where the vertical bending introduces no torsional motion. Figure 3 shows the measurement setup to determine the position of the elastic axis. A fixed-free blade, spanning a length of about 1,450 mm, with a loading fixture near the tip is constructed for this purpose. Only the uniform portion of the blade is considered for the elastic axis measurement. The position of external loading is varied along the chord using a sliding mechanism attached to the loading fixture. The displacement is measured using a stochastic black-white pattern bonded to the surface of the loading block and two optical cameras installed over the top of test apparatus (see Figure 3). Once the measurement setup is finished, the external load is applied first at the quarter chord position and the displacements (translation and rotation) of each mark in the pattern are traced by using a photogrammetric system (Figure 4). Next, the chordwise position of loading is shifted toward leading-edge and trailing-edge so that the exact location of the elastic axis is sought by a linear interpolation. In order to ensure the repeatability of the measurements, the amount of loading is varied. It is found that the measured elastic axis of the blade uniform section is positioned at 27.2 mm (0.225*c*) referenced from the leading-edge. It is noted that the previous HART II estimations predict at 24.9 mm (0.206*c*) [1].

3.2 Section stiffness

The flap bending stiffness is measured separately for the uniform region and the root region. For both cases, a dynamic loading through an excenter rotating with 0.3 Hz is applied by the pulley system to avoid creeping behavior of the glass-fiber composite blade. The elastic axis position is the point of application of the load resulting in a pure bending without any torsion. Figure 5 shows the test setup to measure the blade flap bending in the uniform section of H2A blade. To this purpose, the blade is clamped near the root region located at 23% radial station of the rotor. The displacements at the blade tip under the dynamic load are measured using the photogrammetric system as mentioned above. The flap bending stiffness EI is obtained using the relation given by:

$$EI = \frac{F \cdot L^3}{3 \cdot \Delta} \quad (1)$$

where F is the applied load, L the length between the clamp and the loading block, and Δ the resulting bending displacement. The measured flap bending in the uniform section is found to be 224.2 N-m² as opposed to the previously estimated value of 250 N-m² [1]. It is remarked that the measured value for the equivalent HART II blade (H2E) is 220.9 N-m² which is very close to that of H2A. To determine the flap bending of H2E blade, the three-point bending technique is adopted [4].

The root region of HART II blades has irregular section profiles with a spanwise taper. To find the displacements and the section bending stiffnesses over the non-uniform region, the blade surface is painted with stochastic patterns. Once again, the pure bending loads are applied to the blade and the images of the patterns under different loading conditions are analyzed to determine the section displacements. Figure 6 shows the image processing results using the photogrammetric system subjected to a free of loading and a load of 13.9 N, respectively. It is observed that the initially-uniform color of the images is changed into layers of different colors along the blade span, indicating pure bending deflections. Figure 7 shows the measured deflections of the blade root region as well as the curve-fitted results using the cubic-spline interpolation scheme under different loading conditions (9.83 N and 13.9 N). The bending stiffnesses over the root region are determined by averaging the values

obtained between the two loadings.

The torsion stiffnesses in either the uniform section or the root section are measured using the same test setup as the flap bending, except a static torsion moment applied at the blade tip. The resulting torsion stiffness in the blade uniform region is found to be 146.1 N-m^2 . Note that the previously-estimated value is 160 N-m^2 . The chord bending stiffness is measured only for H2E blade using the three-point bending technique (Figure 8). Both lead-bending and lag-bending stiffnesses are obtained and averaged for the chord bending stiffness, leading to $5,404 \text{ N-m}^2$.

3.3 Mass properties

The mass and inertia properties are determined by a non-destructive testing technique using the computer tomography (CT) facility of DLR (German Aerospace Center) in Stuttgart (Figure 9) due to the fact that the HART II blades are not allowed for chopping them up. The details of the CT-scan and the post-processing procedures yielding segmented images and the follow-on section mass property extraction can be found in Schultz et al. [6]. The resolution of the images obtained using the CT-scan is 0.08288 mm per pixel. Figure 10 shows the CT-scan image and the segmented image for the blade uniform section. From the segmented image, the location of C.G. (center of gravity) and the polar mass moment of inertia (MOI) for the blade section is obtained to be 28.1 mm measured from the leading edge and 0.000791 kg-m based from the C.G., respectively.

Table 1 summarizes the measured blade properties for each of the blades used in the test as compared with the existing HART II records found in the HART II documentation [1]. Figures 11 and 12 show the comparison of the spanwise distributions on stiffness and mass properties between the present measured data and the previous HART II records.

3.4 Rotor natural frequencies

The structural dynamics behavior of HART II rotor in a vacuum condition is investigated using the comprehensive rotorcraft analysis code, CAMRAD II [7]. The blade structure is discretized into 15 nonlinear beam finite elements. Each beam segment is represented by three translational (axial, flap, and lead-lag) and three corresponding rotational degrees of freedom (DOF), resulting in a fifteen DOF per beam finite element. A five degree collective pitch setting is used for the rotating blade analysis.

In Figure 13, the predicted natural frequencies of HART II rotor obtained using the newly measured structural properties are compared against the measured frequencies [8] as well as previous HART II predictions. The continuous solid lines represent the present predictions while the dashed lines indicate the predictions by the previously-available blade properties and the hollow circles denote the measured non-rotating frequencies taken from Ref. 8. The frequencies are non-dimensionalized by the rotor nominal speed ($\Omega = 1041 \text{ RPM}$). It is remarked that the pitch bearing stiffness of $1,700 \text{ N-m/rad}$ is used to match the first measured torsion frequency of the instrumented blade, denoted in Figure 13 as a hollow red circle. The predicted rotating frequencies show only small deviations up to the first torsion frequencies, however, they become larger at higher modes. As is seen from Figures 11 and 12, the changes in the blade properties of the root region are the major source of differences in the natural frequencies.

Future investigation will include the comparison of trim angles, blade responses, airloads, and structural loads of HART II rotor in a descending forward flight condition. Special care will be taken whether the newly measured blade properties affect the aeromechanics predictions of the rotor as opposed to the previously computed values. A sensitivity analysis based on the stochastic approach will be conducted to identify the relative

impact of each blade structural parameter on the aeroelastic behavior of the rotor. It should be mentioned that the recently-published results on HART II validation showed generally good to excellent correlations as compared with the wind tunnel test data [9-11]. However, this does not necessarily mean that the measurement of blade properties is never needed. The existing blade property set of HART II rotor estimated using the finite element analysis should be replaced with the accurately measured property data obtained from the original blades and the uncertainties associated with the blade structural properties should be resolved.

References

1. van der Wall, B. G., "2nd HHC Aeroacoustic Rotor Test (HART II) – Part I: Test Documentation," Institute Report IB 111-2003/31, German Aerospace Center (DLR), Braunschweig, Germany, 2003.
2. van der Wall, B. G., "A Comprehensive Rotary-Wing Data Base for Code Validation," *The Aeronautical Journal*, Vol. 115, No. 1164, Feb. 2011, pp. 91-102.
3. Wöndle, R., "Calculation of the Cross Section Properties and the Shear Stresses of Composite Rotor Blades," *Vertica*, Vol. 6, 1982, pp. 111-129.
4. Jung, S. N., and Lau, B. H., "Determination of HRT I Blade Structural Properties by Laboratory Testing," NASA-CR-2012-216039, NASA Ames Research Center, Aug. 2012.
5. Jung, S. N., You, Y. H., Lau, B. H., Johnson, W., and Lim, J. W., "Evaluation of Rotor Structural and Aerodynamic Loads Using Measured Blade Properties," *Journal of the American Helicopter Society*, Vol. 58, No. 4, Oct. 2013.
6. Schulz, M., Opitz, S., and Riemenschneider, J., "A New Concept to Determine the Mass Distribution of an Active Twist Rotor Blade," *CEAS Aeronautical Journal*, Vol. 3, Nos. 2-4, Dec. 2012, pp. 117-123.
7. Johnson, W., *CAMRAD II: Comprehensive Analytical Model of Rotorcraft Aerodynamics and Dynamics*, Johnson Aeronautics, Palo Alto, CA, 1992.
8. van der Wall, B. G., Lim, J. W., Smith, M. J., Jung, S. N., Bailly, J., Amiraux, M., and Boyd, Jr., D. D., "The HART II International Workshop: An Assessment of the State-of-the-Art in Comprehensive Code Prediction," *Aeronautical Journal*, Vol. 4, No. 3, Sept. 2013, pp. 223-252.
9. Smith, M. J., Lim, J. W., van der Wall, B. G., Baeder, J. D., Biedron, R. T., Boyd, Jr, D. D., Jayaraman, B., Jung, S. N., and Min, B. Y., "The HART II International Workshop: An Assessment of the State-of-the-art in CFD/CSD Prediction," *Aeronautical Journal*, published online, Aug. 2013 (doi: 10.1007/s13272-013-0078-8).
10. Jung, S. N., Sa, J. H., You, Y. H., Park, J. S., and Park, S. H., "Loose Fluid-Structure Coupled Approach for a Rotor in Descent Incorporating Fuselage Effects," *Journal of Aircraft*, Vol. 50, No. 4, July 2013, pp. 1016-1026.
11. You, Y. H., Sa, J. H., Park, J. S., Park, S. H., and Jung, S. N., "Modern Computational Fluid Dynamics/Structural Dynamics Simulation for a Helicopter in Descent," *Journal of Aircraft*, Vol. 50, No. 5,, Sept. 2013, pp. 1450-1464.

Table 1 Summary of blade property table for the uniform section.

Properties	Existing HART	Present Measured		
	II data	H2A	H2S	H2E
Elastic axis, mm	24.9	27.2	-	-
C.G., mm	30.4	-	28.1	27.2
Flap bending, N-m ²	250	224.2	-	220.9
Chord bending, N-m ²	5,200	-	-	5,404
Torsion stiffness, N-m ²	160	146.1	-	-
Mass per unit length, kg/m	0.95	-	0.948	-
Polar mass MOI, kg-m	0.000747	-	0.000791	0.000792

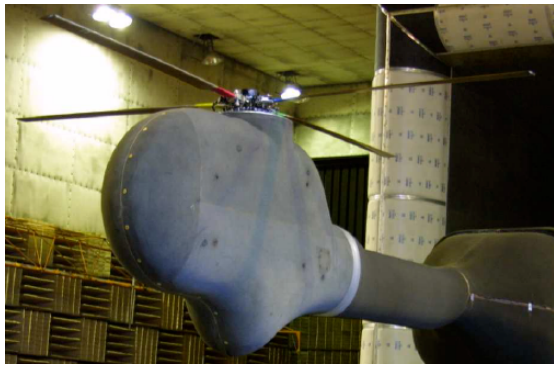


Fig. 1 HART II rotor in the wind tunnel (2002).



(a) Instrumented HART II blade (H2A)



(b) HART II spare blade (H2S)



(c) Equivalent HART II blade (H2E)

Fig. 2 HART II blades used in the property test.

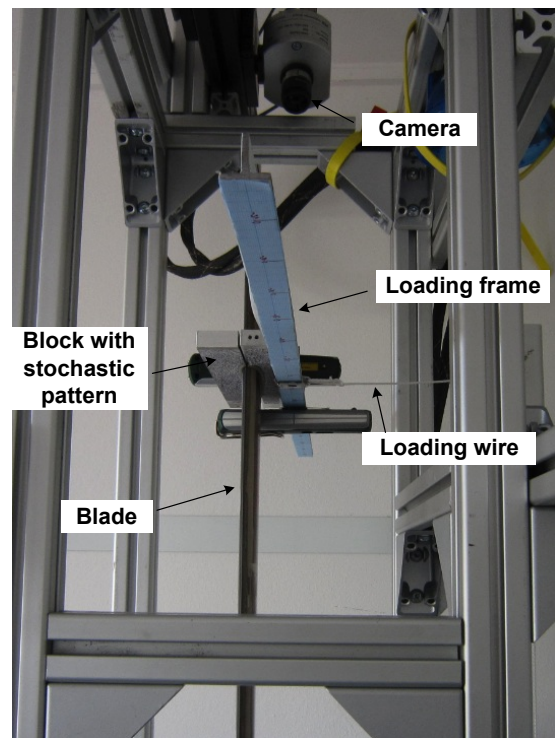


Fig. 3 Measurement setup for the elastic axis.

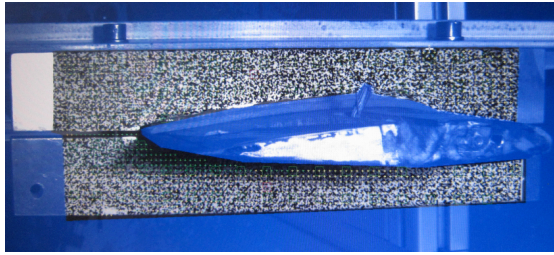
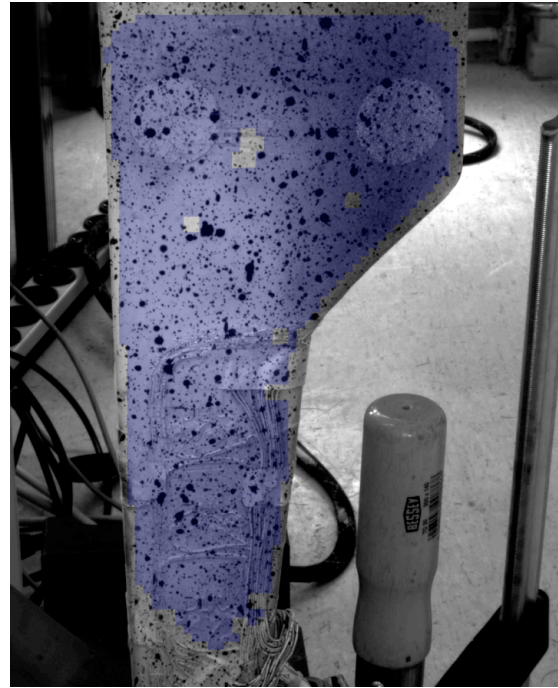


Fig. 4 Display of photogrammetric system.



Fig. 5 Test setup for blade stiffness measurements.



(a) Unloaded case



(b) Loaded case with 13.9 N.

Fig. 6 Photogrammetric process results over the blade root region.

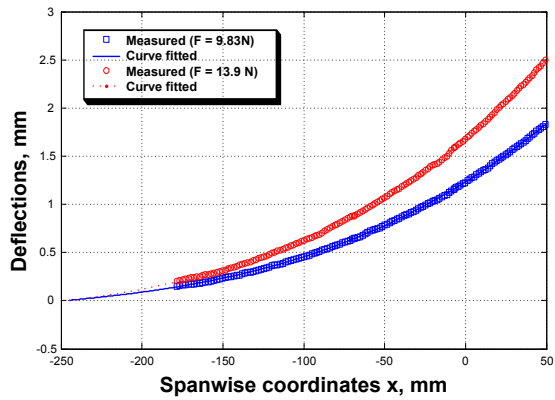


Fig. 7 Blade displacements of the root region under pure bending loads.



Fig. 8 Three-point bending test for chord-bending stiffness.

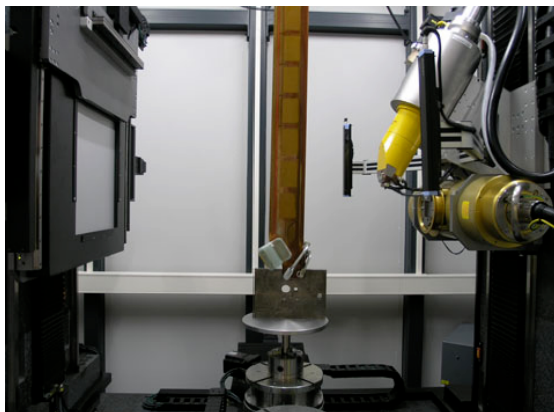
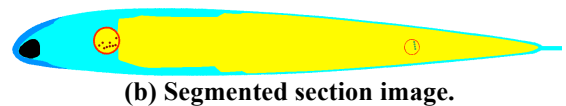


Fig. 9 Computer tomography setup of DLR (German Aerospace Center) in Stuttgart [6].

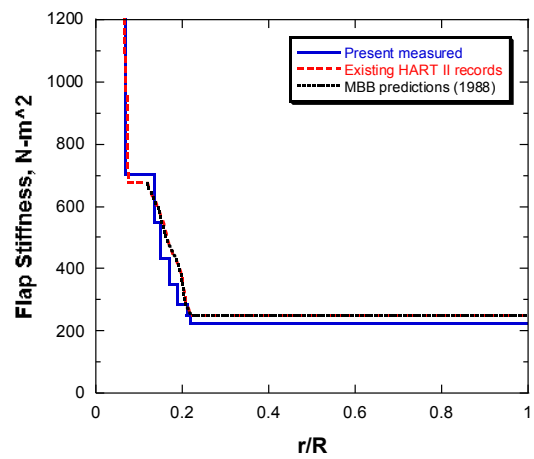


(a) CT-scan image

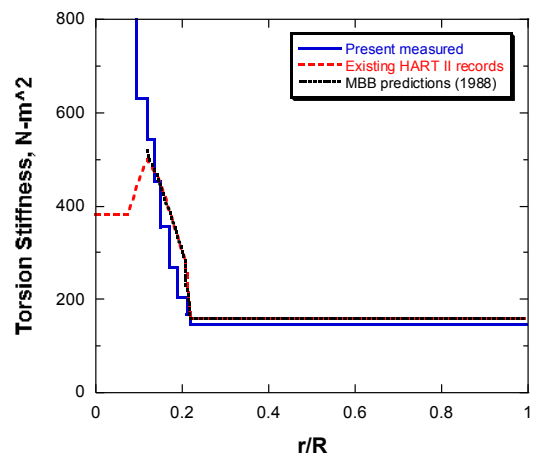


(b) Segmented section image.

Fig. 10 CT section image and its segmentation for blade uniform section.

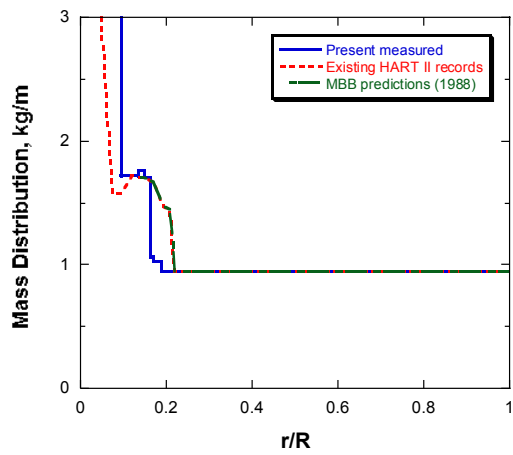


(a) Flap bending

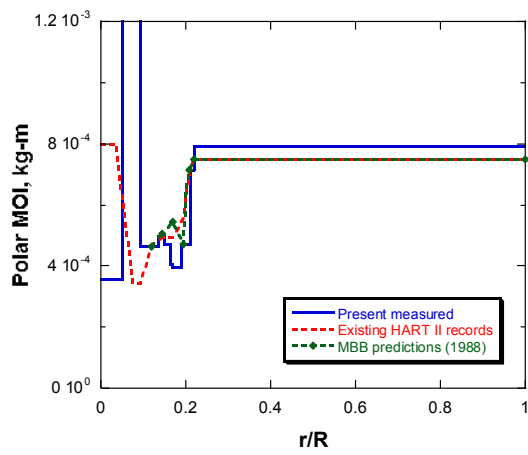


(b) Torsion stiffness

Fig. 11 Measured stiffness properties of HART II blades.



(a) Mass distribution



(b) Polar mass moment of inertia

Fig. 12 Measured mass properties of HART II blades.

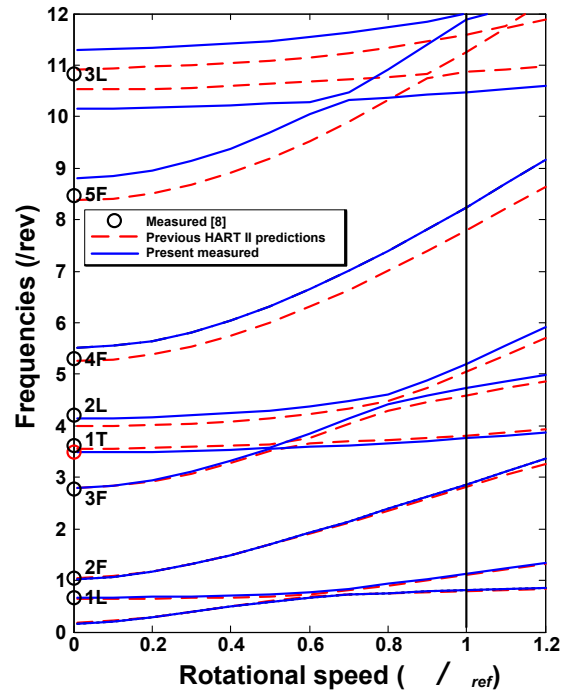


Fig. 13 Comparison of rotating natural frequencies.